EXPERIMENTAL ANALYSIS OF CRITICAL VOID RATIO CONCEPT IN ARTIFICIALLY CEMENTED SANDS

by

Gilberto S. Reyes

Project Report submitted to the Faculty of the

Virginia Polytechnic Institute and State University

in partial fulfillment of the requirements for the degree of

MASTER OF ENGINEERING

in

Civil Engineering

APPROVED:

G.Wayne Clough, Chairman

L. C. Rude

T. Kuppusamy

October, 1983
Blacksburg, Virginia

DEDICATION

To Eileen ...

ACKNOWLEDGEMENTS

The author wishes to express his sincere gratitude to the members of his committee for their continued assistance : Dr. L. C. Rude, Dr. T. Kuppusamy, and especially to Dr. G. Wayne Clough, for his important role as chairman, and for his guidance in the preparation of this project.

The author is deeply indebted to the Ministry of Public Works and Highways (MPWH), Philippines, and the International Road Federation (IRF) for without their scholarship this graduate study would not have been possible.

Grateful acknowledgement is given to the respondents who shared their experiences and knowledge. The encouragement and support of his friends and colleagues have been most helpful.

Special thanks and appreciation are due to Mr. Dante B. Potante for his most needed assistance in the final draft of this manuscript.

Finally, the support and encouragement by the author's parents, Mr. and Mrs. Rizalino G. Reyes, and his brother and sisters, have been deeply appreciated and have made this study possible.

TABLE OF CONTENTS

LIST OF TABLES

LIST OF FIGURES

Chapter I

INTRODUCTION

One of the important studies which is used to evaluate the relation between drained and undrained characteristics of sands is the critical void ratio concept. The critical void ratio is defined as the void ratio at which failure will occur at zero volume change. The concept was first established by Casagrande [1] and following that, a number of methods were suggested for determining this soil characteristic. Several researches have been made to determine the critical void ratios of different types of clean sands but little or no testing has been done on sands with various amounts of cementation.

Cemented sands are found in many areas of the world and one of their distinguishing characteristics is their ability to stand in steep natural slopes. The cementation in the sand is provided by small amounts of agents, such as silica, hydrous silicates, hydrous iron oxides, and carbonates deposited at the points of contact between sand particles. Cementation or cementation-like effects can also be produced by a dense packing of sand grains or by a matrix of silt and clay particles [3].

This investigation was directed primarily towards the analysis of the critical void ratio concept on sand with small amount of cementation. Because of the difficulties in sampling naturally cemented samples, artificially prepared samples were used in this investigation. A total of 16 static triaxial drained tests were performed, following the procedures

developed by Rad,et al. [6] in sample preparation and saturation. Curves were developed to illustrate the static behavior of the samples and the results showed consistency with those of Rad's work. Two methods were presented to determine the critical void ratio for each of the confining pressures used. The critical confining pressures were also determined to develop the critical state line of the fabricated cemented samples.

Chapter II

REVIEW OF CRITICAL VOID RATIO CONCEPT

The nature of the volume changes in sands during shearing, and their relationship to the density of the sand and the confining pressure were placed on a quantitative basis through the detailed studies by Casagrande [1]. He demonstrated that under conditions were volume changes can occur and for any given confining pressure, loose sands compress during shear and dense sands dilate, leading to the postulation of a critical void ratio, e_{crit}, for which no volume change would occur during loading. It was also shown that the critical void ratio is not a constant for any given soil but decreases as the confining pressure increases.

The relationship between volume changes, void ratio and confining pressure in drained tests on a cohesionless material is illustrated in Fig. 1. If a series of drained tests is conducted, using a constant confining pressure, on samples having different void ratios, e_c, after consolidation under the confining pressure, the relationship between volume change at failure and void ratio after consolidation will have the form shown in Fig.1(a). From a plot of this type, the critical void ratio, e_{crit}, that is, the void ratio of a sample for which there is no volume change at failure under the confining pressure used in the test series can readily be determined. If similar series of tests are conducted using other confining pressures, a series of such relationships can be deter-

mined, as shown in Fig.1(b), leading to a series of values for the critical void ratio corresponding to different values of the confining pressure. From these results, a plot can be made to show the variation of the critical void ratio, e_{crit} [7].

Similarly, a series of drained tests could be conducted on samples initially consolidated under different confining pressures but having the same void ratio after consolidation, e_c, under these pressures. In this case, it would be found that the volume change at failure would vary with the confining pressure as shown in Fig.1(d) and it would be possible to establish, for the particular value of void ratio used in the test series, the value of a confining pressure for which there would be no volume change at failure. By analogy with the definition of the term critical void ratio, the confining pressure for which there would be no volume change at failure might be termed the critical confining pressure, σ_{3crit}, corresponding to a particular value of the void ratio after consolidation, e_c. By conducting similar series of tests at different values of e_c, a series of corresponding values of critical confining pressure and void ratio, e_c, could be determined, Fig.1(e), from which the relationship between σ_{3crit}, and e_c could be established as shown in Fig.1(f) [7].

It follows from the definitions of critical void ratio and critical confining pressure that the relationship shown in Figs.1(c) and 1(f) are identical in form. Thus, for samples prepared in the same manner, the relationship between the critical void ratio, e_{crit}, and the confining

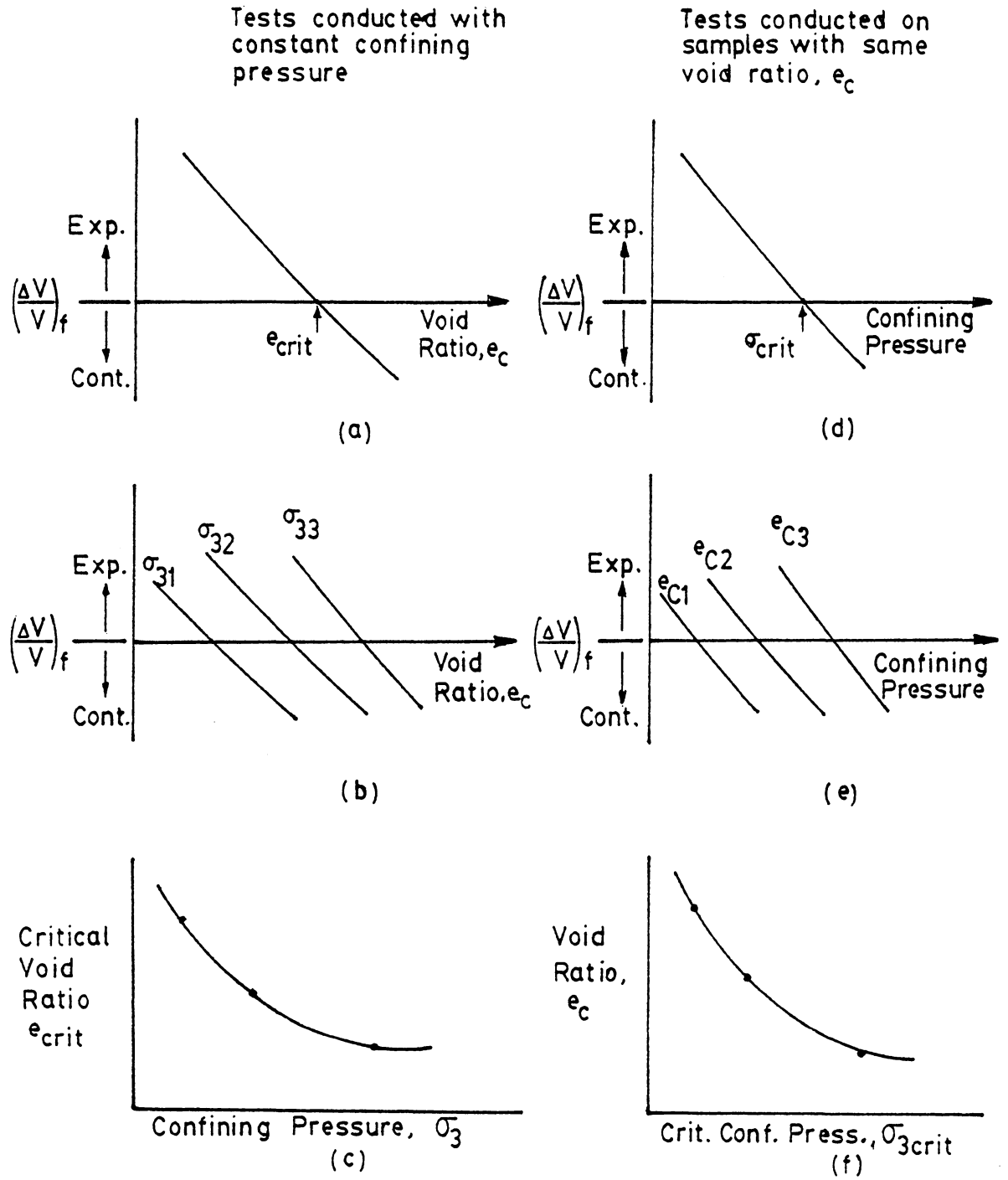

Figure 1: Relationship between Volume Change at Failure, Void Ratio, and Confining Pressure in Drained Tests

pressure under which samples are initially consolidated, σ_{3c}, is also the relationship between the critical confining pressure, σ_{3crit}, and the void ratio after consolidation under the confining pressure, e_c, as shown in Fig. 2 [7].

Another method to determine the critical void ratio is by plotting the void ratio changes during the loading against axial strain as shown in Fig. 3, from the same series of drained tests described above.

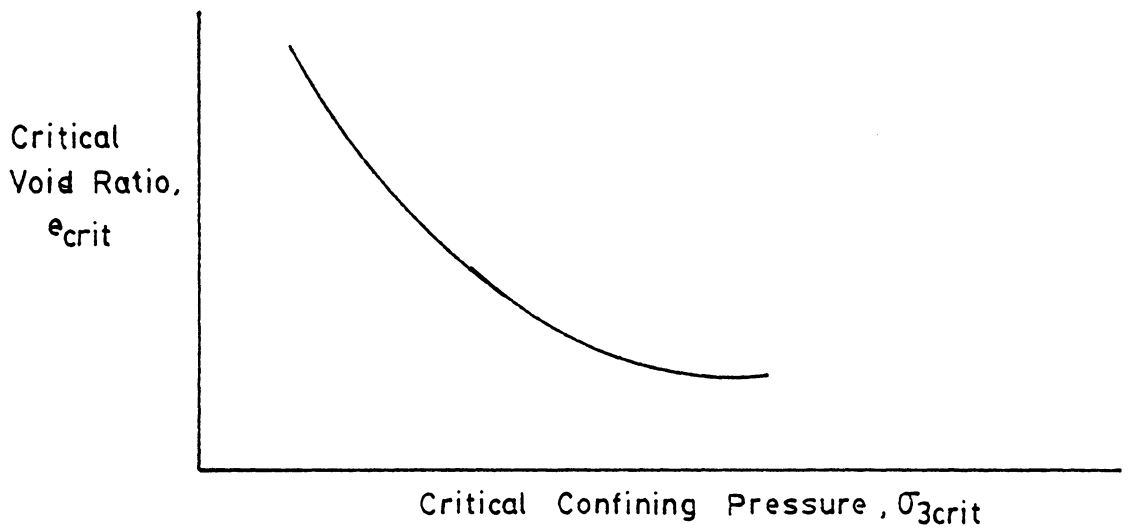

Figure 2: Relationship between Critical Confining Pressure and Void Ratio after Consolidation

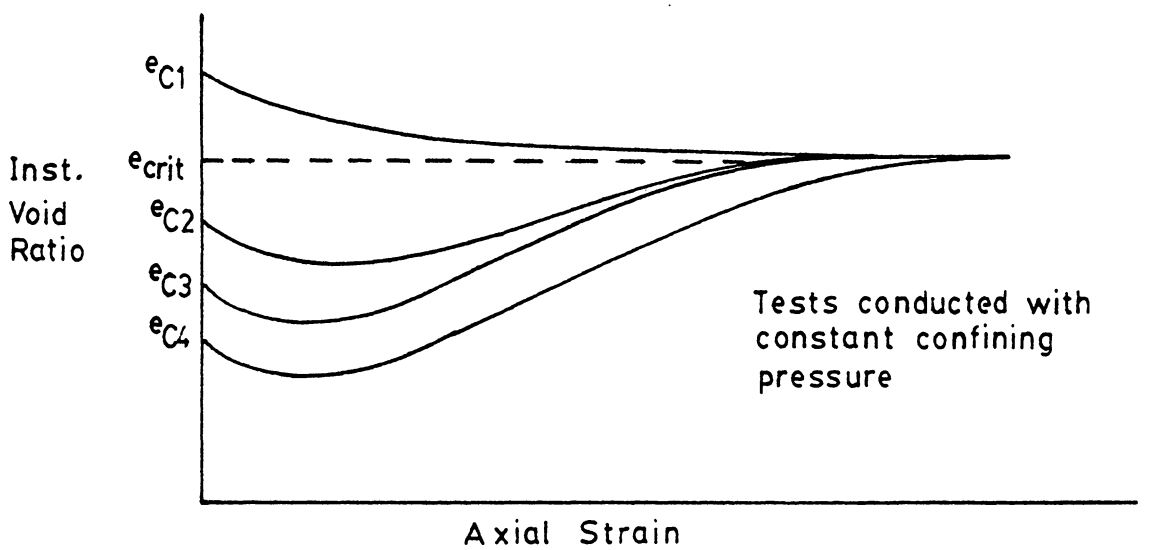

Figure 3: Relationship between Instantaneous Void Ratio And Axial Strain

Chapter III

DESCRIPTION OF TEST SPECIMENS

The static triaxial drained tests were carried out on samples of artificially cemented sands. It has been shown from previous investigations [3, 6] that the artificially prepared samples can simulate the behavior of the naturally cemented sands. Following the work of Rad [6], the samples were prepared using a mixture of processed Monterey Beach Sand No.0 and low alkali Portland cement. Monterey Beach Sand was used as the principal testing medium because it is readily available commercially and a large data base exists for it. It consists mainly of quartz and a lesser amount of feldspar and other minerals. The particles vary in shape from rounded to subangular. The index properties as given in Table 1 are based on existing data [6, 8].

Fig. 4 shows the grain-size distributions for Artificially Cemented Sands with 1 and 2 percent cement, Uncemented Monterey Sand No.0 and Weakly Cemented Sands [6]. The results indicate that the artificially cemented sands with 1 percent cement and the weakly cemented soils have relatively similar distributions with relatively uniform particles.

TABLE 1

Index Properties of Uncemented and Cemented Monterey Sand No.0

Index Property	Uncemented	Cemented (c =1%)
Max. Dry Unit Weight (pcf)	105.70	105.70
Min. Dry Unit Weight (pcf)	89.30	89.30
Max. Void Ratio	0.85	0.85
Min. Void Ratio	0.56	0.56
Specific Gravity	2.65	2.65
D10 (mm)	0.28	0.28
D50 (mm)	0.36	0.36
D60 (mm)	0.40	0.40
D60/D10	1.43	1.43
Sand	Fine	Fine

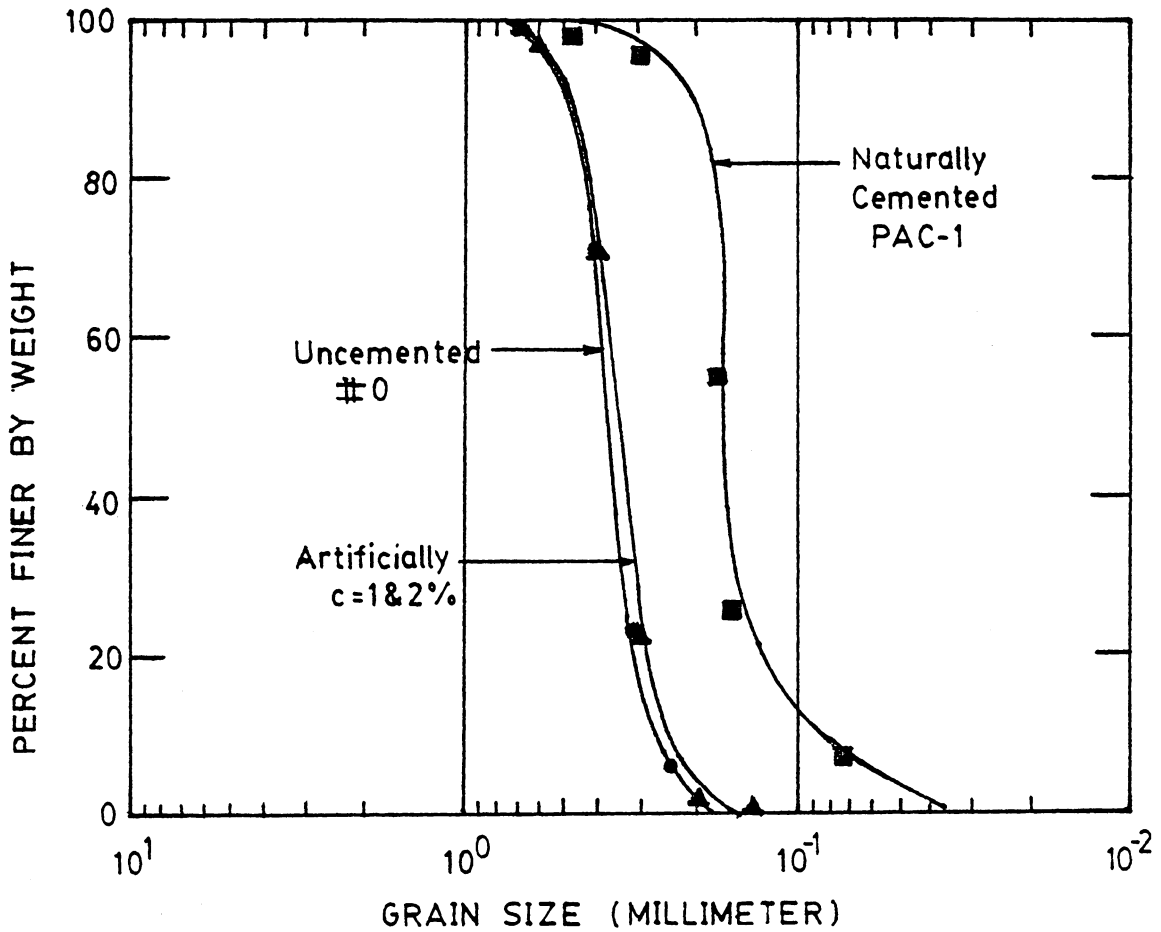

Figure 4: Grain-Size Distribution of Uncemented Monterey Sand No.0, Artificially Cemented Sand and Naturally Cemented Sand

Chapter IV

SAMPLE PREPARATION

Since weak and loose specimens were needed to carry out this study, the following steps were taken in making the samples with 1 percent cement:

1. Cylindrical plexiglass molds with a narrow longitudinal split on one side are used. The molds are 70 2 mm in diameter, and 147 1 mm high. Initially the mold is cleaned, its internal diameter measured and the internal surface thoroughly coated with silicon lubricant. An aluminum or plexiglass cap, which has four holes equally spaced on the perimeter of a concentric 5 cm diameter circle, is then placed in the bottom and the split is kept closed using three hose clamps. The diameter of each hole is approximately 10 mm. A coarse filter paper on top of a fine wire mesh is placed on the bottom cap inside the mold to prevent the passage of the sands and/or cement. After this the mold is weighed.
2. 1000 gm of air dried Monterey sand No.0, is placed in a mixing bowl.
3. 10 gm of dry Portland cement (Type I-II, low alkali) is weighed out corresponding to 1 percent of the dry weight of the sand.
4. 4 gm of water (0.4 percent of the dry weight of the sand) is spread on the sand which is then stirred for 60 seconds (pre-

ferrably by an electrical mixer). This creates a slight moisture in the surface of the sand.

5. While the sand is being mixed, the cement is added slowly to the sand and the mixing is continued thereafter for another 60 seconds.

6. The sand-cement mixture is further agitated using a rubber spatula for 30 seconds. This leads to a coating of the sand particles by cement; no segregation between the cement and sand is observed.

7. An amount of sand-cement, depending upon the desired relative density of the sample and the volume of the mold, is weighed. This volume of sand- cement is placed in a flask with its rim plugged by a rubber cork with a 5 mm hole in it. The mixed material is allowed to flow into the mold by inverting the flask, as shown in Fig. 5. The distance of fall from the flask is maintained at 5 cm.

8. Should higher densities than that obtained by pouring only be desired, the mold is rotated at approximately 5 rpm and tapped with a steel ruler by hand while the sand is dropping. By changing the amount of tapping, different relative densities could be obtained.

9. The top of the sample is leveled and the mold is then weighed to recalculate the relative density of the sample. A coarse filter paper is placed on top of the sample and an aluminum plexiglass cap without holes is placed on top of the mold.

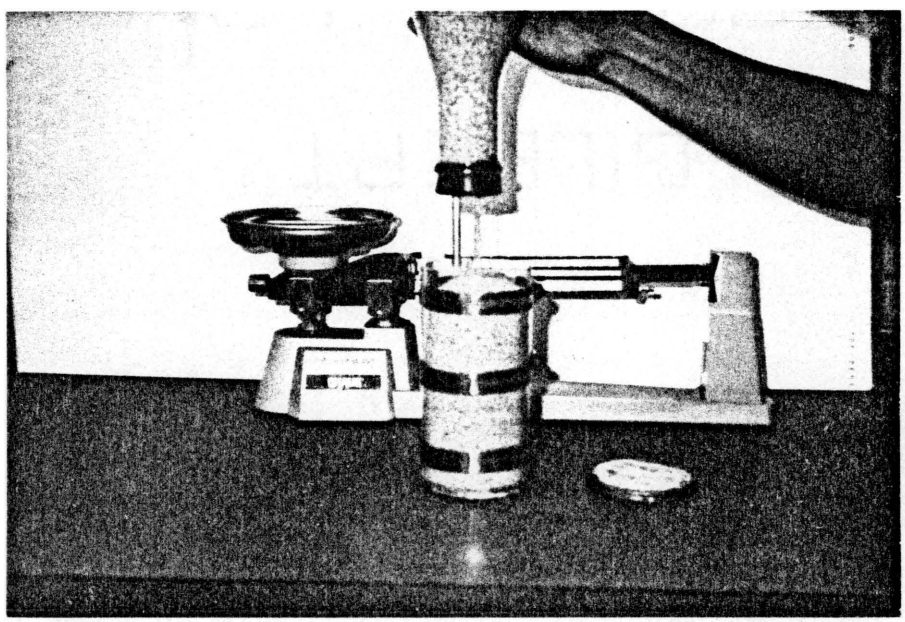

Figure 5: Procedure for Manufacturing Samples of Artificially Cemented Sands with 1% Cement

10. The mold is placed in a styrofoam container on top of a thin layer of coarse sand which allows free drainage of water through the holes in the bottom cap to the sample.
11. Water is introduced to the container such that the water level in the container rises approximately 1.5 mm per minute. The sample is completely submerged in approximately 2 or 3 hours, and a small settlement occurs at the top due to the breakdown of capillary tension and possible particle rearrangement.
12. The container and the sample are then placed in a humid room for curing. After 14 days the sample is extruded by removing the hose clamps and the longitudinal split pushed open so that the sample slides freely from the mold on top of a porous stone. The first few centimeters from the top and the bottom are trimmed off as a cautionary action to avoid higher concentrations of cement. The sample stands by itself when extruded from the mold.
13. The sample is weighed out, the dimensions measured and prepared for placing in the triaxial cell for testing.

The steps enumerated above follow the procedures developed by Rad [6] with some modifications done in this investigation.

Chapter V

SAMPLE SATURATION

All samples in this investigation were saturated by a new procedure called the "Vacuum Procedure" since it had been found out that cemented sands were very difficult to saturate by conventional back-pressure techniques, and the use of carbon dioxide can lead to unwanted reactions of the soil cementing agents with it. A theoretical basis for this new saturation technique was established by Rad, et al.[6] and they presented experimental evidence to confirm its utility.

Fig. 6 schematically shows the equipment arrangement used in this investigation for saturating a sample with the vacuum procedure. The following steps are taken:

1. Place the specimen with a membrane around it inside the triaxial cell.
2. Fill up the upper reservoir (UR) with deaired water, while the lower reservoir (LR) is kept empty.
3. Apply an initial increment of vacuum valve to the top of the sample (valve 4 is open). Valve 3 which controls access to the bottom of the sample is closed at this time.
4. Apply an increment vacuum inside the TX cell,outside the sample. This vacuum should be less than the vacuum inside the sample. Thus, a negative back-pressure system is established, with the difference between vacuum at point A and B the effective stress applied on the sample.

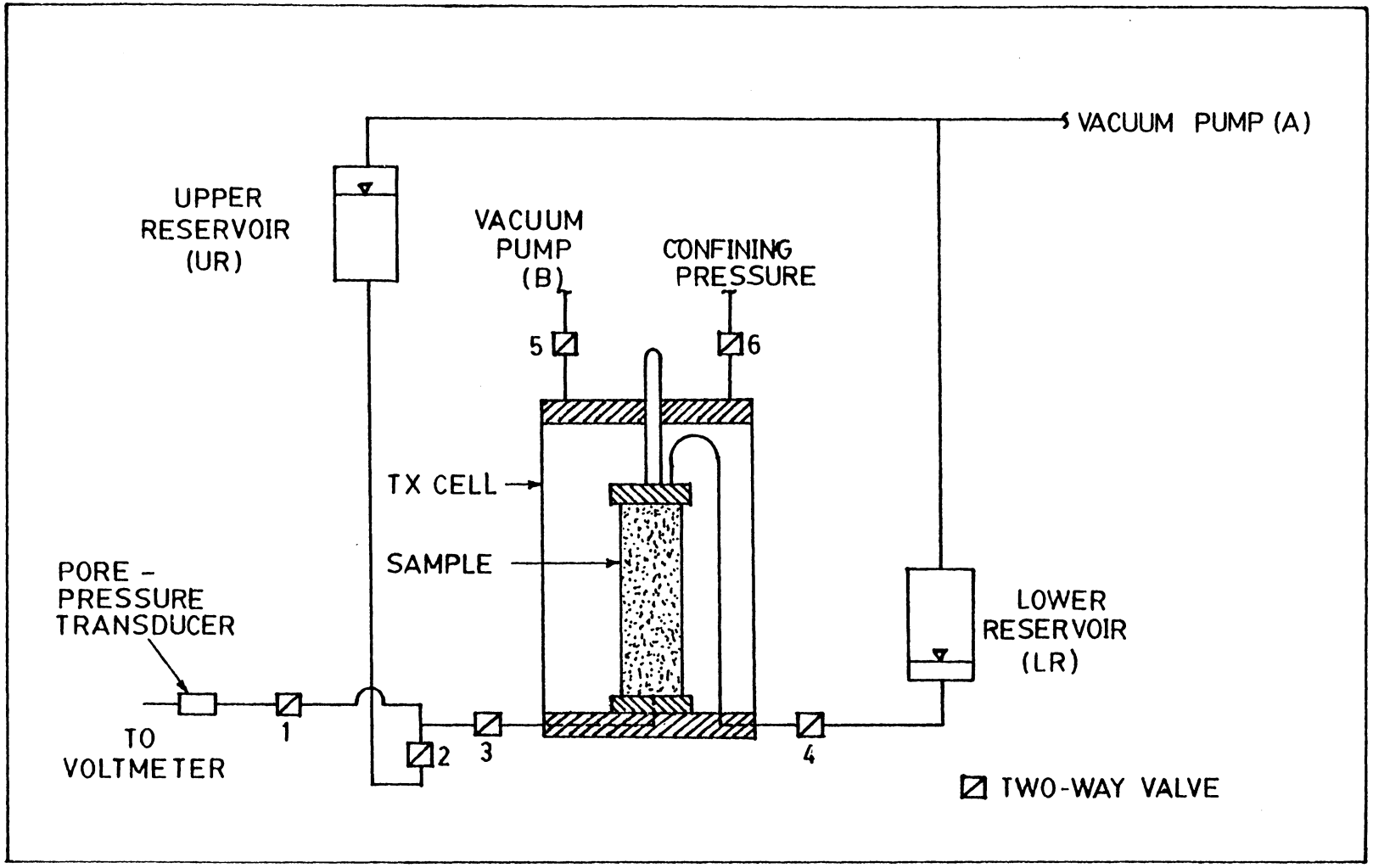

Fig. 6 Equipment arrangement for saturating soil specimen using the vacuum procedure

5. Increase the vacuum at point A (inside the sample) while the same increase is applied at point B (outside the sample), till the desired level of vacuum is reached.
6. Maintain the vacuum for a short period of time, depending upon the grain size and initial degree of saturation of the sample.
7. Percolate water through the sample by opening valves 2 and 3; water is drawn from the sample into the lower reservoir until the sample is nominally saturated (valve 1 is closed).
8. Close valve 2 and continue the application of the vacuum inside and outside the sample for a period of 1-5 minutes in order to insure a proper equilibrium inside the sample.
9. Close valve 4 in order to isolate the sample from the reservoirs and open valve 1.
10. Decrease the vacuum (increase the absolute pressure) at point B (outside the sample). This action results in an increase in the total confining stress. Measure the induced change in pore water pressure (ΔU) using the pore-pressure transducer, and calculate the pore pressure coefficient B [9].
11. Decrease the vacuum inside the sample by adjusting the vacuum pump at point A till the difference between the pressures inside and outside the sample are at the desired effective stress level.
12. Continue the process described in steps 9-11 until the desired degree of saturation or B value is achieved. Of course, once

the vacuum on the inside of the specimen is reduced to zero, the confining pressure in the cell will now be positive in order to keep a small effective stress in the soil. Any subsequent back-pressuring which may be necessary follows the normal positive back-pressure procedures.

Chapter VI

DESCRIPTION OF TESTING PROCEDURES

6.1 SPECIMEN PREPARATION

After curing for 14 days, the sample was extruded from the mold and prepared for setting up in the triaxial cell. The following steps were taken in preparing the test specimens :

1. Place the extruded sample and the porous stone on the bottom platten of the triaxial cell. Apply silicon lubricant around the bottom platten to ensure no leakage will occur.
2. Fit four rubber O-rings over a membrane stretcher and roll them to near the middle of its length, Fig. 7. Fit a rubber membrane inside the suction member stretcher and fold back the ends over the outside of the stretcher tube so that the membrane is not wrinkled or twisted, Fig.7(b).
3. Apply vacuum through the small tube attached to the membrane stretcher, so as to draw the membrane tightly against the inside wall of the stretcher tube.
4. While maintaining the vacuum, carefully lower the device over the specimen, Fig.7(c). When the stretcher is positioned centrally over the specimen, release the vacuum so that the membrane clings to the specimen.
5. Roll the membrane bottom end gently on to the bottom platten, making a smooth fit with no entrapped air. Hold the membrane

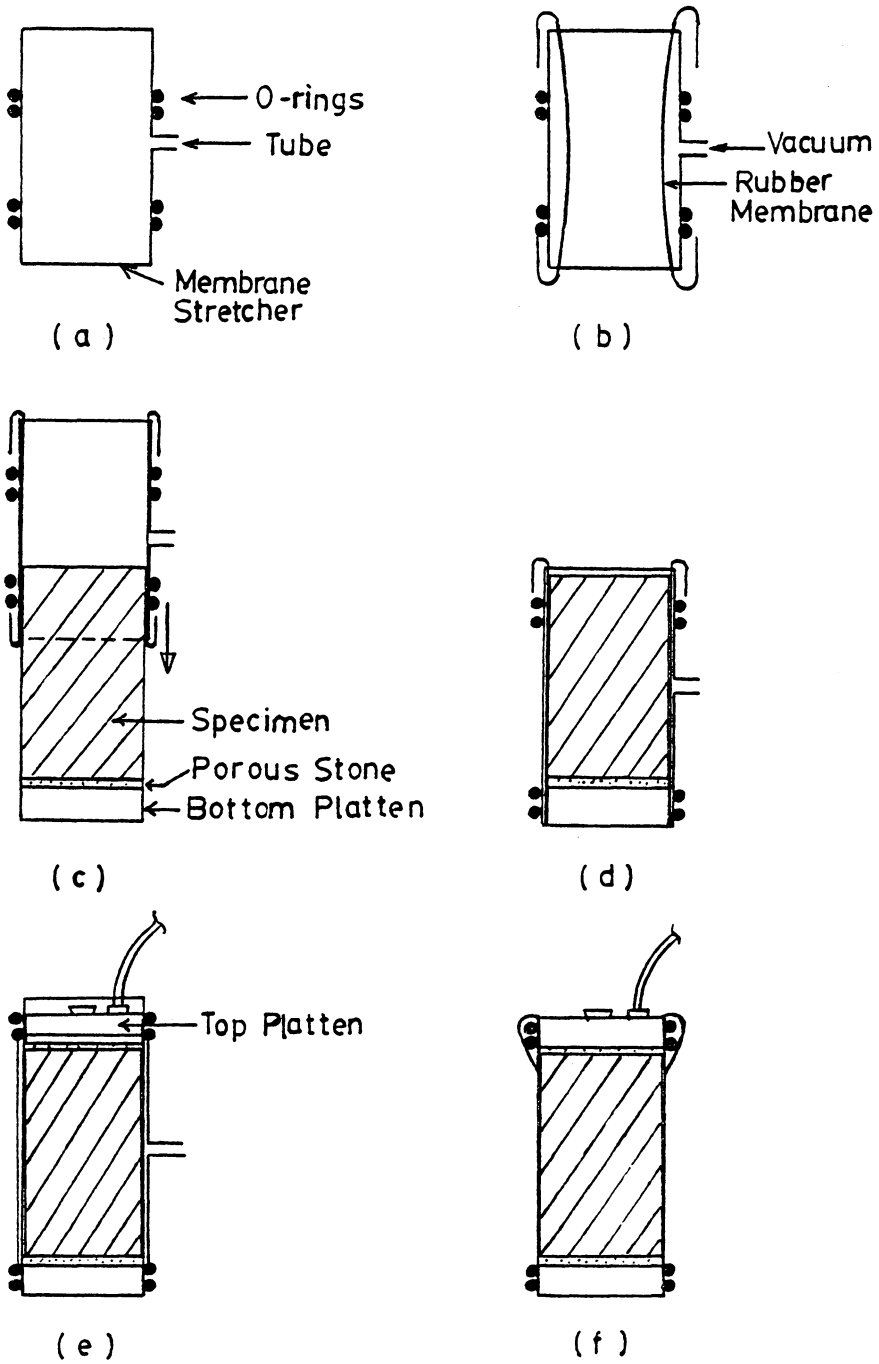

Figure 7: Stages of Fitting Rubber Membrane to Specimen

stretcher steady with one hand,and roll off two of the O-rings to seal the membrane on to the bottom platten, Fig.7(d).

6. Place a porous stone on top of the sample and place the top platten over the porous stone. Repeat the operation in step 5 to seal the top cap, Fig.7(e).
7. Remove the stretcher and fold back the top end of the membrane neatly over the sealing rings, Fig.7(f).
8. Place the lucite cylinder and the specimen is ready for saturation and triaxial testing.

6.2 TEST PROGRAM

Sixteen strain-controlled drained triaxial loading tests were performed on saturated samples using the triaxial equipment and pore pressure panel as shown in Fig. 8. All of the samples were saturated using the vacuum procedure,as described in chapter V. The triaxial cell was then connected to the pore pressure panel for further saturation of the sample by back pressure technique. Each sample was consolidated under the confining pressure until no significant volume changes were observed. High confining pressures were applied to attain volumetric contraction at failure. Volume changes were measured from a calibrated burette attached to the pore pressure panel, Fig. 9. Volume changes during consolidation were recorded to calculate the initial void ratio of the samples before the application of the deviator stress. The pore pressure, which is equal to the back pressure applied, was monitored

by a pressure transducer attached to the pore pressure line of the panel. The transducer was connected to a voltmeter which converts pressure into equivalent voltage. The samples were loaded at a strain rate of 15% per hour to prevent changes in pore pressure in the sample during the loading. Load and volume change readings corresponding to the predetermined deformation readings were recorded, the deformation being read from a dial gage attached at the cross bar of the triaxial equipment. Normal loads were measured by a load cell attached to the piston of the triaxial equipment and which is connected to a voltmeter that converts the load being applied into equivalent voltage. The load cell used in this investigation has a maximum capacity of 2000 lbs and has a calibration factor of 66.445 lbs per mv. The tests were continued until deviator stress increased significantly or until 25% axial strain was reached.

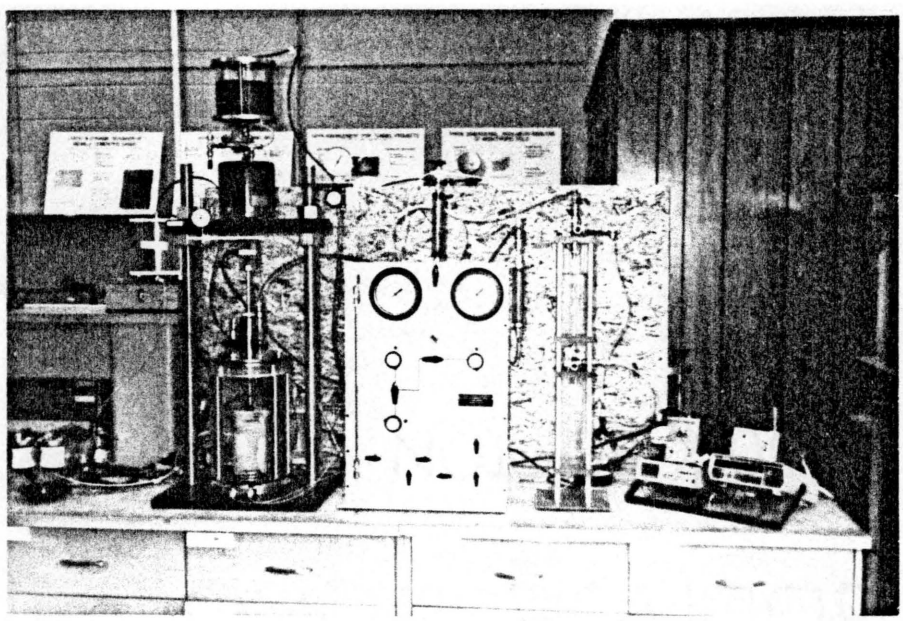

Figure 8: Equipment Set-up for Triaxial Testing

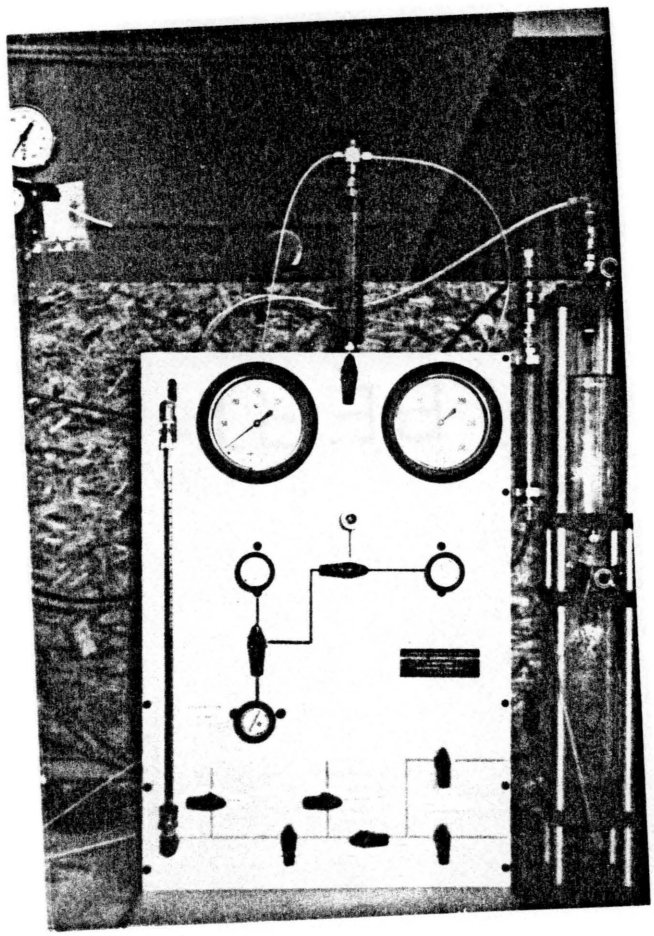

Figure 9: Pore Pressure Panel

Chapter VII

DISCUSSION AND ANALYSIS OF TEST RESULTS

7.1 RESPONSE TO DRAINED LOADING

Typical stress-strain and volume change curves together with void ratio- axial strain curves are shown in Fig. 10 to Fig. 13. The results of the tests are given in Table 2. The basic trends observed for the stress-strain and volume change data are consistent with information previously reported by Clough,et al. [3] and Mitchell [5]. The results show that increasing the confining pressure increases the strength of the samples, as well as the slopes of the initial portions of the stress-strain curves. The samples exhibited ductile behavior and there is a transition to a more ductile response as the confining pressures increase. This behavior is due to the contribution of frictional resistance which becomes dominant for weakly-cemented sands at high confining pressures [6]. The more the contribution of frictional component of strength, the more ductile response results.

The figures also reveal that volumetric expansion decreases as the confining pressures increase. One of the interesting phenomena noted in the figures is the dilatant behavior of the loose samples even at high confining pressures up to 95 psi. The reason for this is thought to be the formation of the cementation crystals in the voids which decrease the void space [6]. This, in essence, makes the artificially cemented sand specimens behave as if they are denser than would be indicated by the relative density established before crystallization .

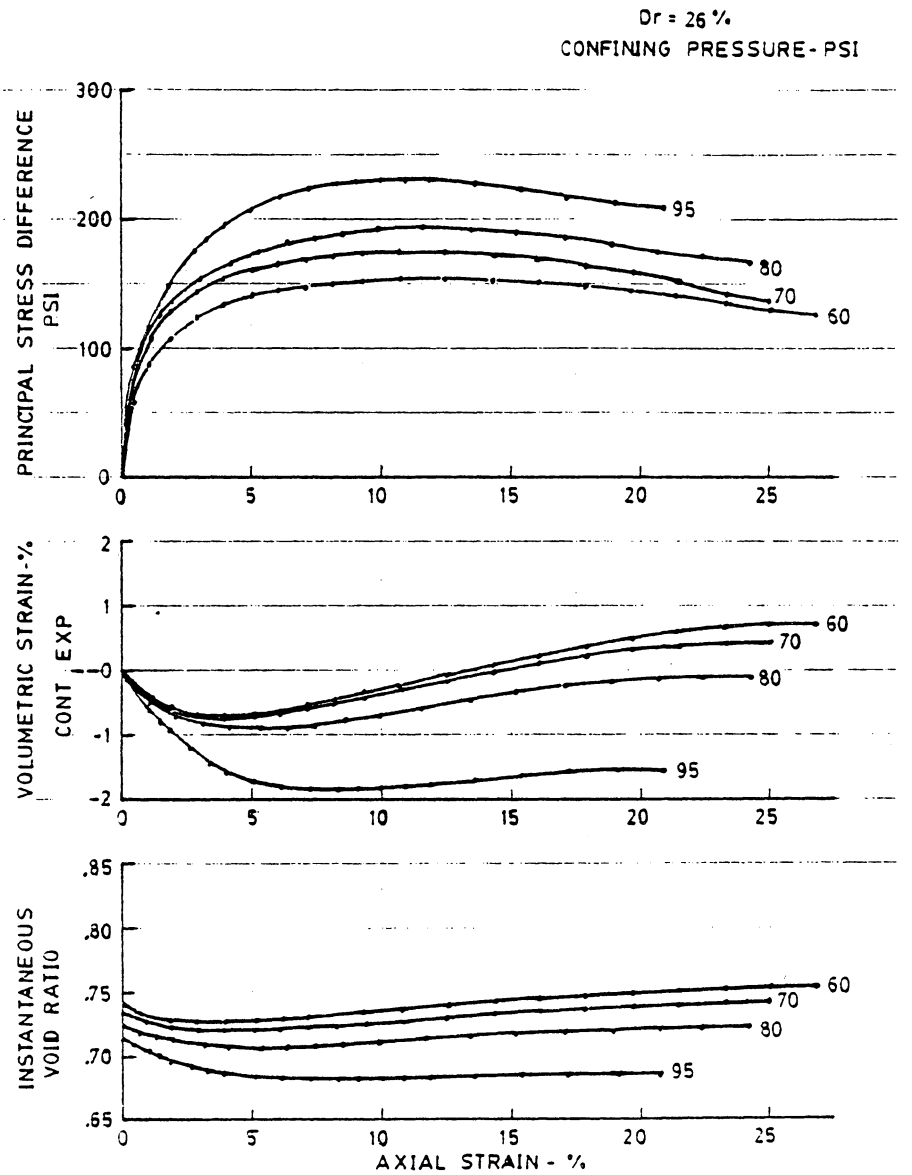

Figure 10: Stress-Strain Curves for Artificially Cemented Sands with 1% Cement, Relative Density = 26%

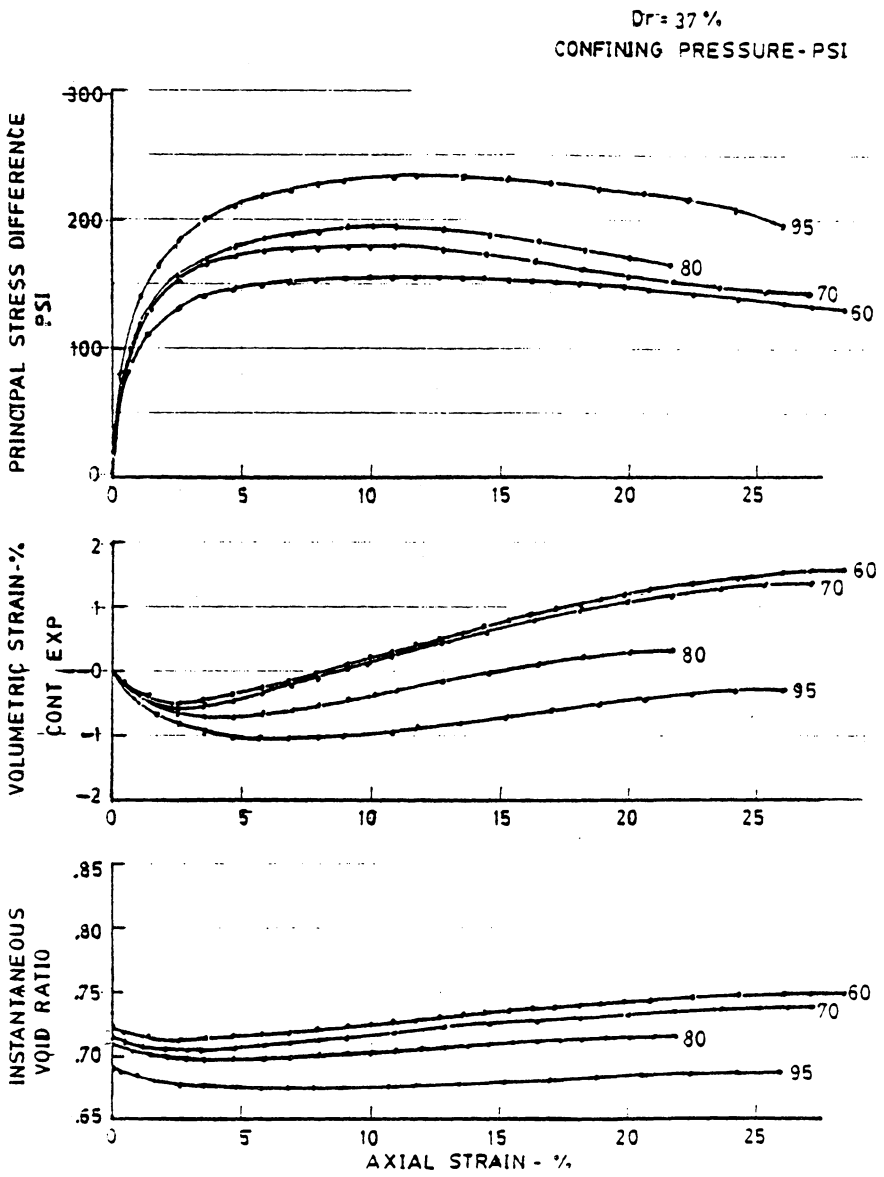

Figure 11: Stress-Strain Curves for Artificially Cemented Sands with 1% Cement, Relative Density = 37%

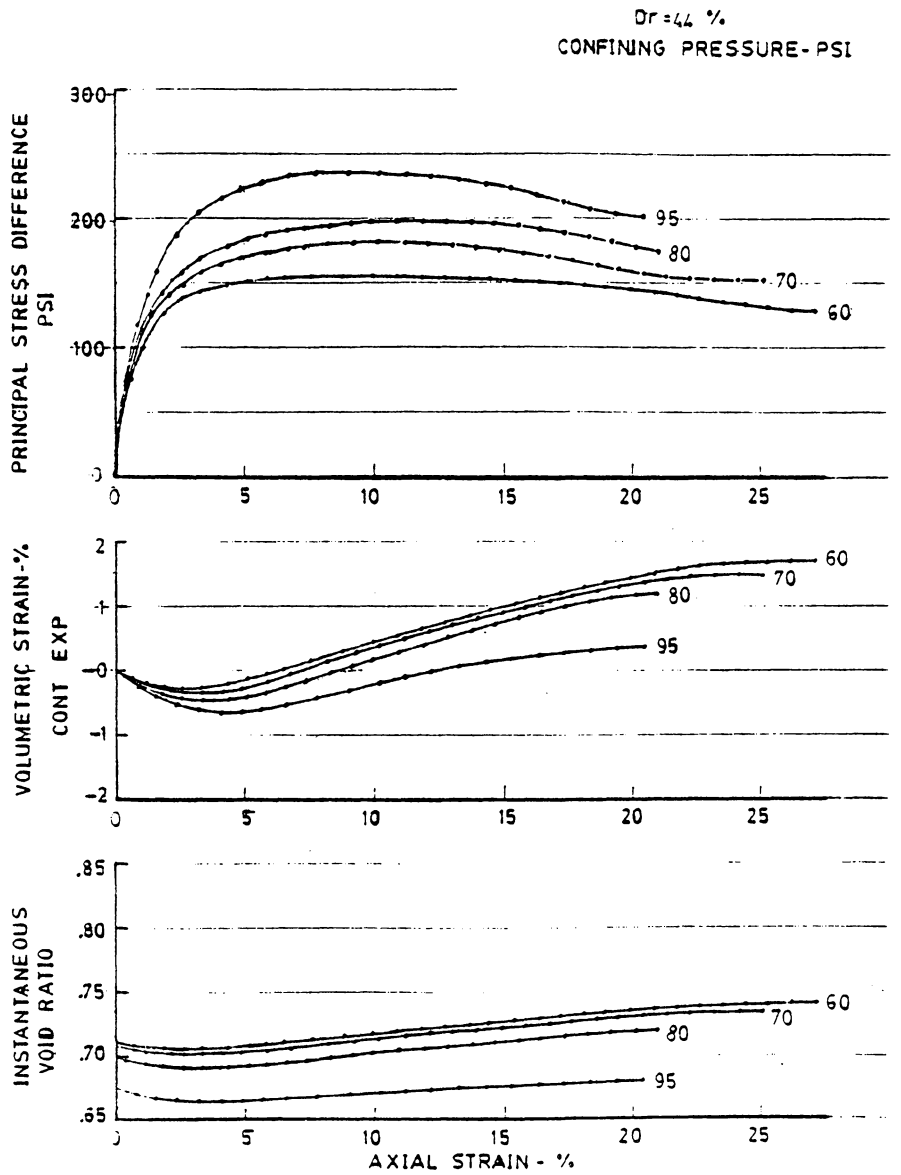

Figure 12: Stress-Strain Curves for Artificially Cemented Sands with 1% Cement, Relative Density = 44%

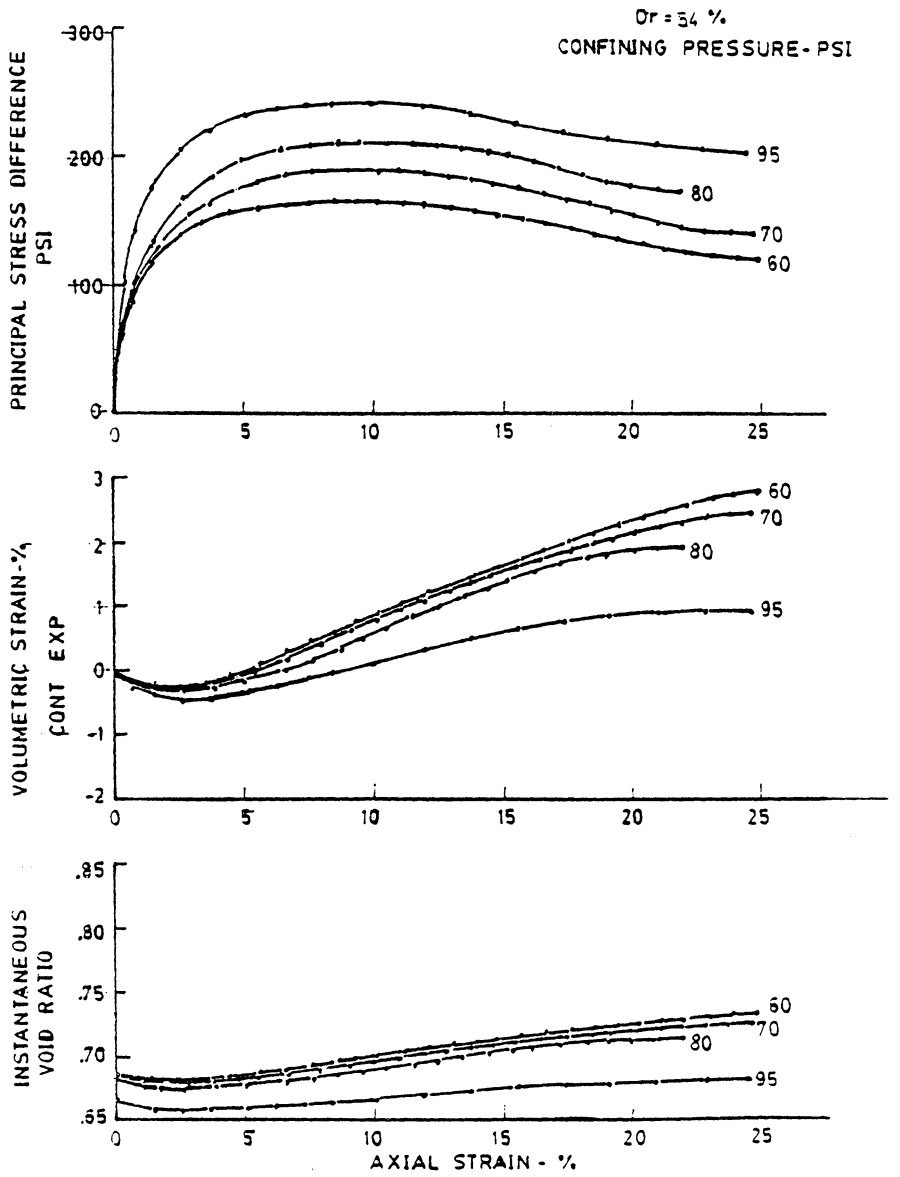

Figure 13: Stress-Strain Curves for Artificially Cemented Sands with 1% Cement, Relative Density = 54%

TABLE 2

Results of Static Triaxial Tests on Artificially Cemented Sands with 1% Cement, Monterey Sand No. 0

Sample No.	Dr* %	σ'_3 psi	Peak Strength		
			Axial Strain %	$\sigma_1-\sigma_3$ psi	Volume Change %
1	25.6	60	11.63	153.45	-0.17
2	26.3	70	10.75	174.65	-0.31
3	26.9	80	11.60	193.63	-0.60
4	26.6	95	11.79	230.10	-1.78
5	37.4	60	11.72	155.41	+0.39
6	38.0	70	9.94	178.60	+0.17
7	37.7	80	10.94	194.27	-0.30
8	36.8	95	11.66	233.27	-0.90
9	44.4	60	10.85	156.46	+0.53
10	43.7	70	10.21	181.56	+0.42
11	44.7	80	10.96	198.66	+0.28
12	45.0	95	9.37	236.47	-0.26
13	55.0	60	10.14	164.05	+0.90
14	54.4	70	10.05	188.26	+0.80
15	54.1	80	10.50	208.51	+0.68
16	54.8	95	10.03	240.19	+0.11

* Design relative density

Fig. 14 shows the peak strength values for the samples, plotted in the form of q-p diagram with coordinates of $(\sigma_1-\sigma_3)/2$ versus $(\sigma_1 + \sigma_3)/2$. The figure reveals that the samples exhibit a cohesion intercept which increases as the relative density increases. This is due to the fact that as the relative density increases the contact surface between the particles increases and, therefore, better and stronger cementation bonds can form [6]. Similarly, the friction angle also increases as the relative density increases. Comparing the results of the tests on samples, with those of Rad's results as shown in Fig. 15, both investigations obtained the same values of friction angles of 38 and 54 degrees for relative densities of 26% (Rad's 25%) and 54% (Rad's 50%) respectively. However, this investigation obtained slightly greater cohesion intercepts at 0.8 psi and 1.4 psi.

7.2 CRITICAL VOID RATIO

Fig. 16(a) shows the relationship between the volumetric strain at failure and the initial void ratios of the samples after consolidation under confining pressures of 60, 70, 80, and 95 psi. Failure points were determined from the peak of the stress-strain curves. By interpolating data points, the critical void ratios corresponding to the confining pressures used were determined, as follows :

Confining Pressure (psi)	e_{crit}
60	0.735
70	0.722

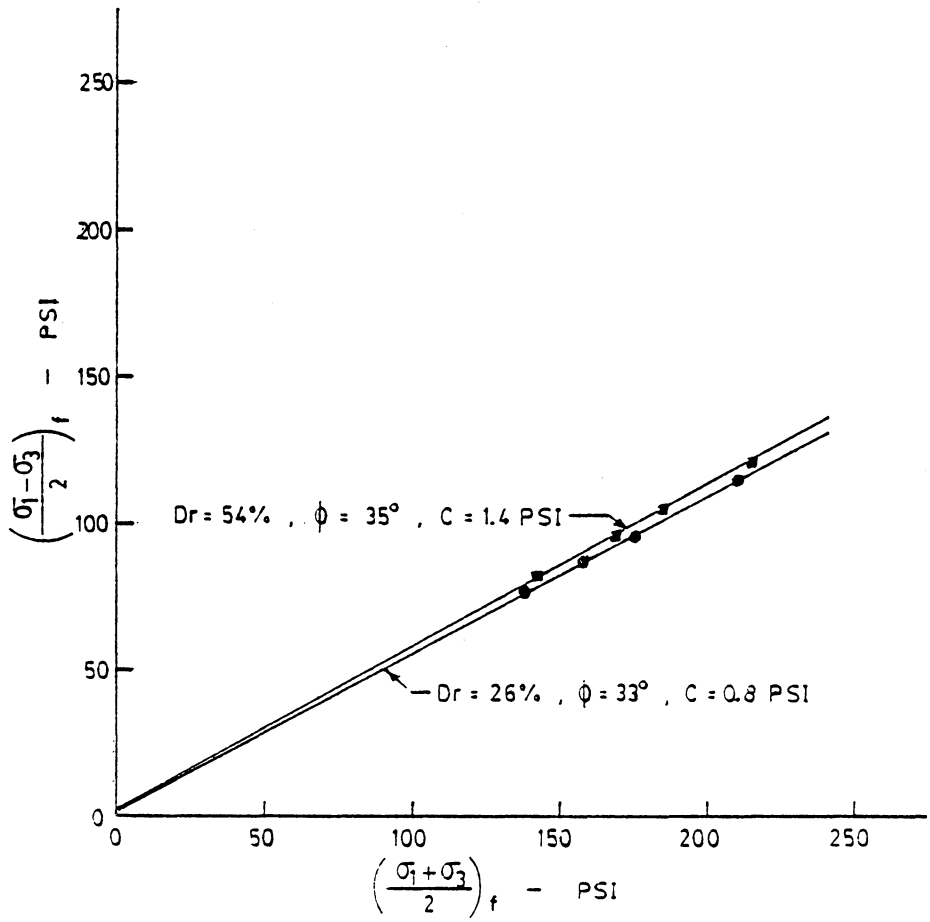

Figure 14: Peak Strength Envelopes for Artificially Cemented Sand Samples with 1 % Cement, Relative Density =26% & 54%

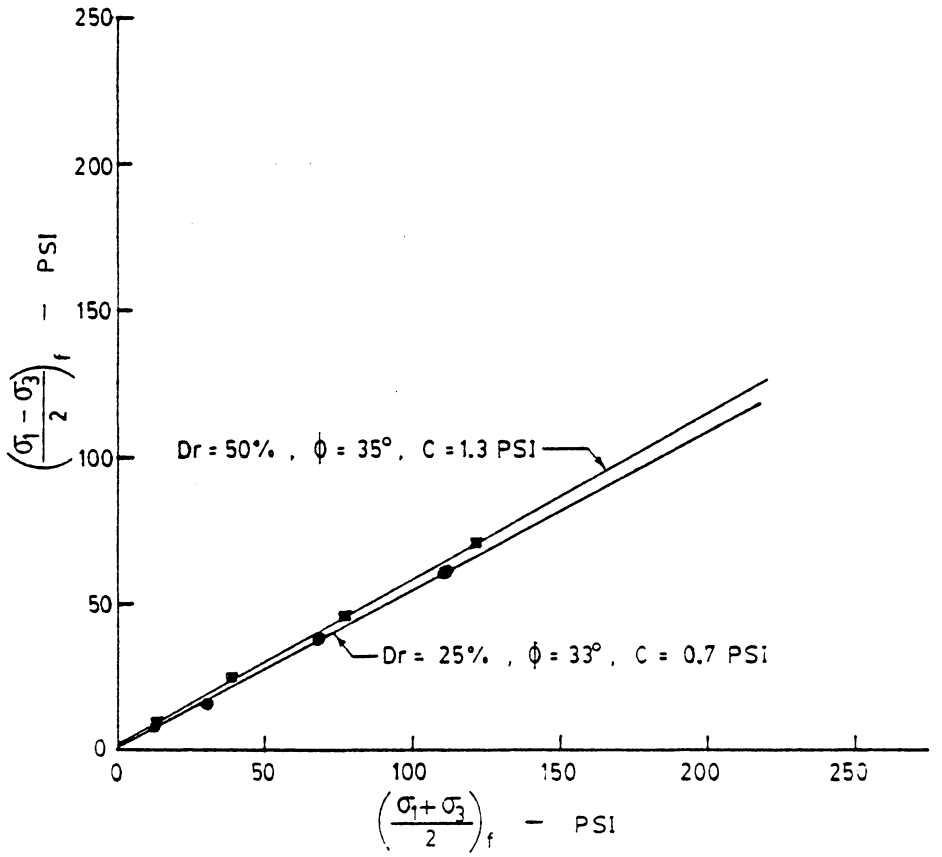

Figure 15: Peak Strength Envelopes for Artificially Cemented Sand Samples with 1% Cement, Relative Density = 25% & 50% (Rad)

80	0.703
95	0.668

As expected, the value of the critical void ratio decreases as the confining pressure increases.

As a comparative analysis, the void ratio changes during the loading are plotted against axial strains, as shown in Fig. 17 to Fig. 20 for samples prepared at relative densities of 26%, 37%, 44% and 54%. By taking the average values of the void ratios where the curves levelled off, the following values of critical void ratio were obtained.

Confining Pressure (psi)	e_{crit}
60	0.745
70	0.735
80	0.715
95	0.685

It may be observed that the values obtained from this method are different from the first method. This is expected since this method depends on the accuracy of the tests at strain levels beyond 20%. Beyond this point the specimen becomes severely distorted and further readings have little meaning [4]. The expected convergence of the curves into a common value of critical void ratio in each confining pressure used was not attained, therefore, using the values obtained from this method would not be reliable.

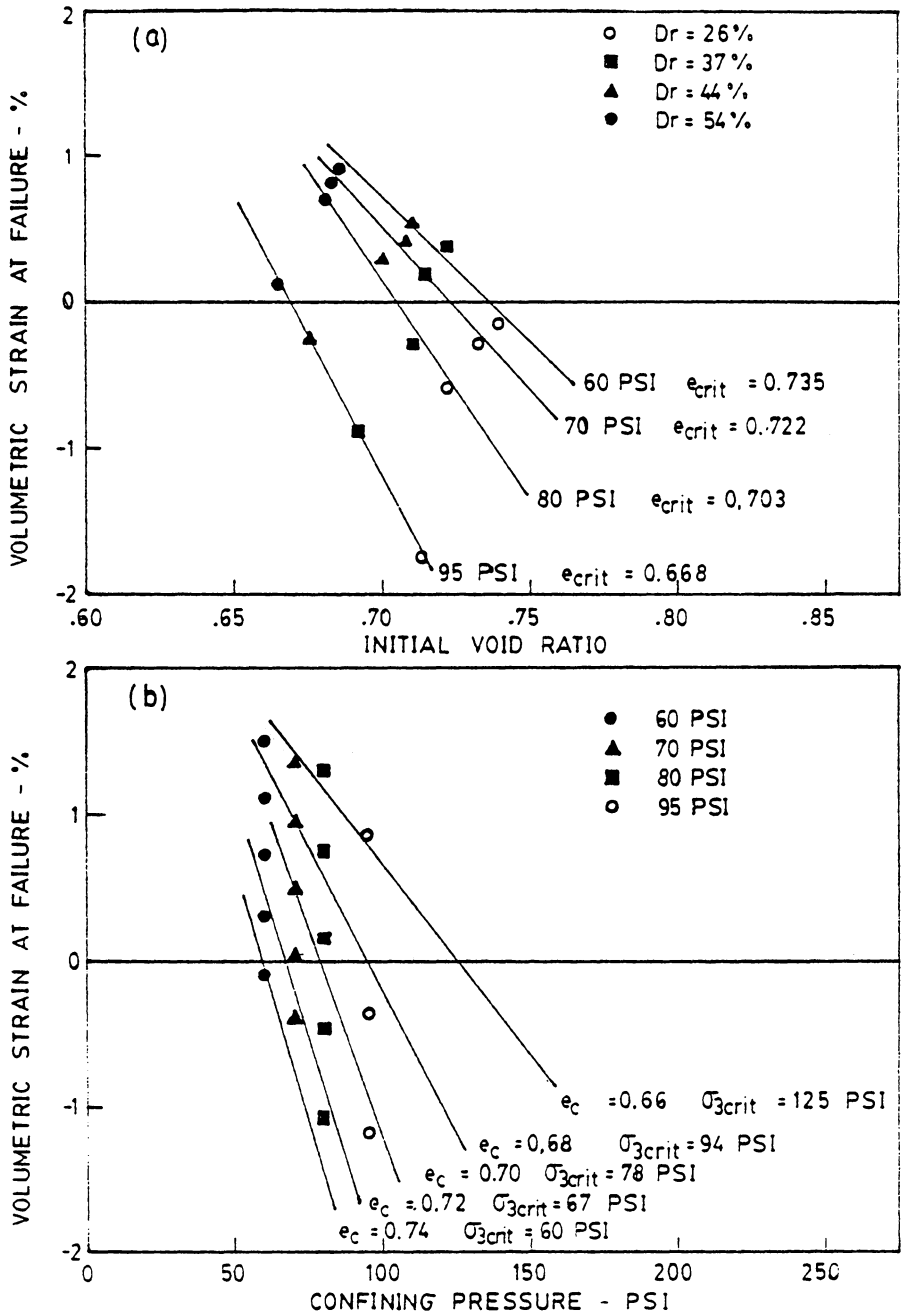

Figure 16: Relationship between Volumetric Strain at Failure, Initial Void Ratio and Confining Pressure

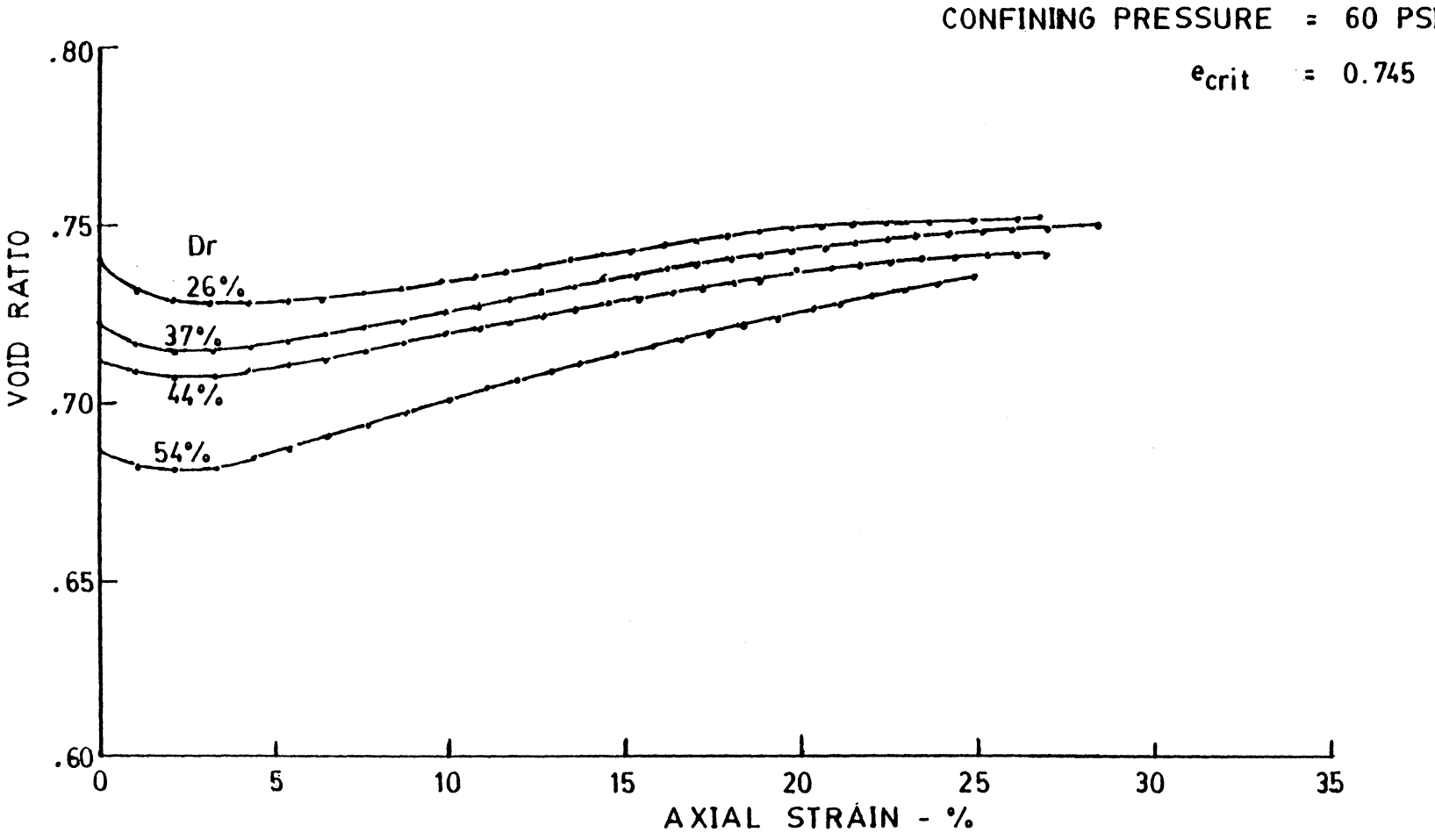

Fig.17 - Void Ratio - Axial Strain Curves for Artificially Cemented Sand with 1 Percent Cement , Confining Pressure = 60 PSI

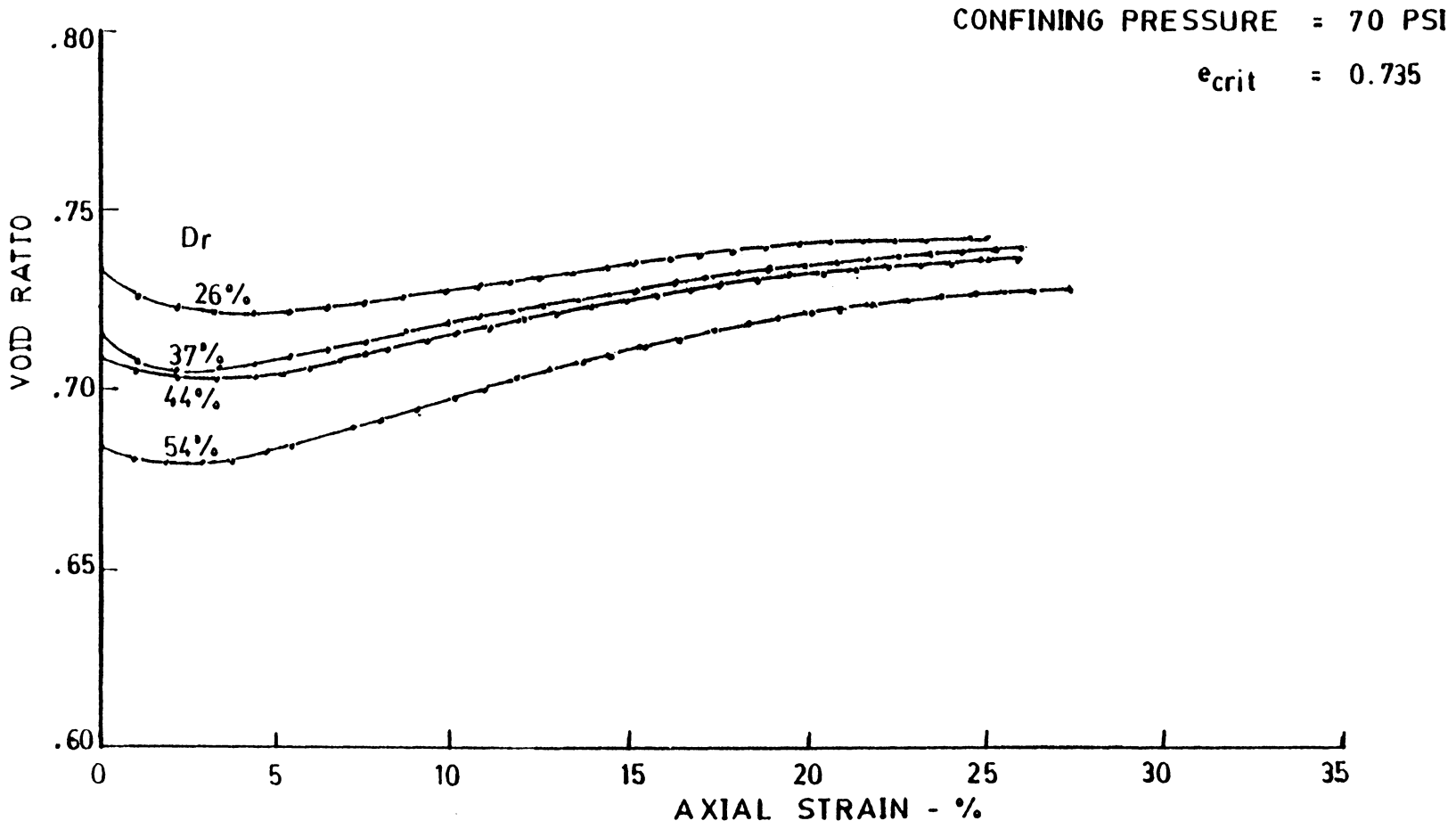

Fig.18 – Void Ratio – Axial Strain Curves for Artificially Cemented Sand with 1 Percent Cement, Confining Pressure = 70 PSI

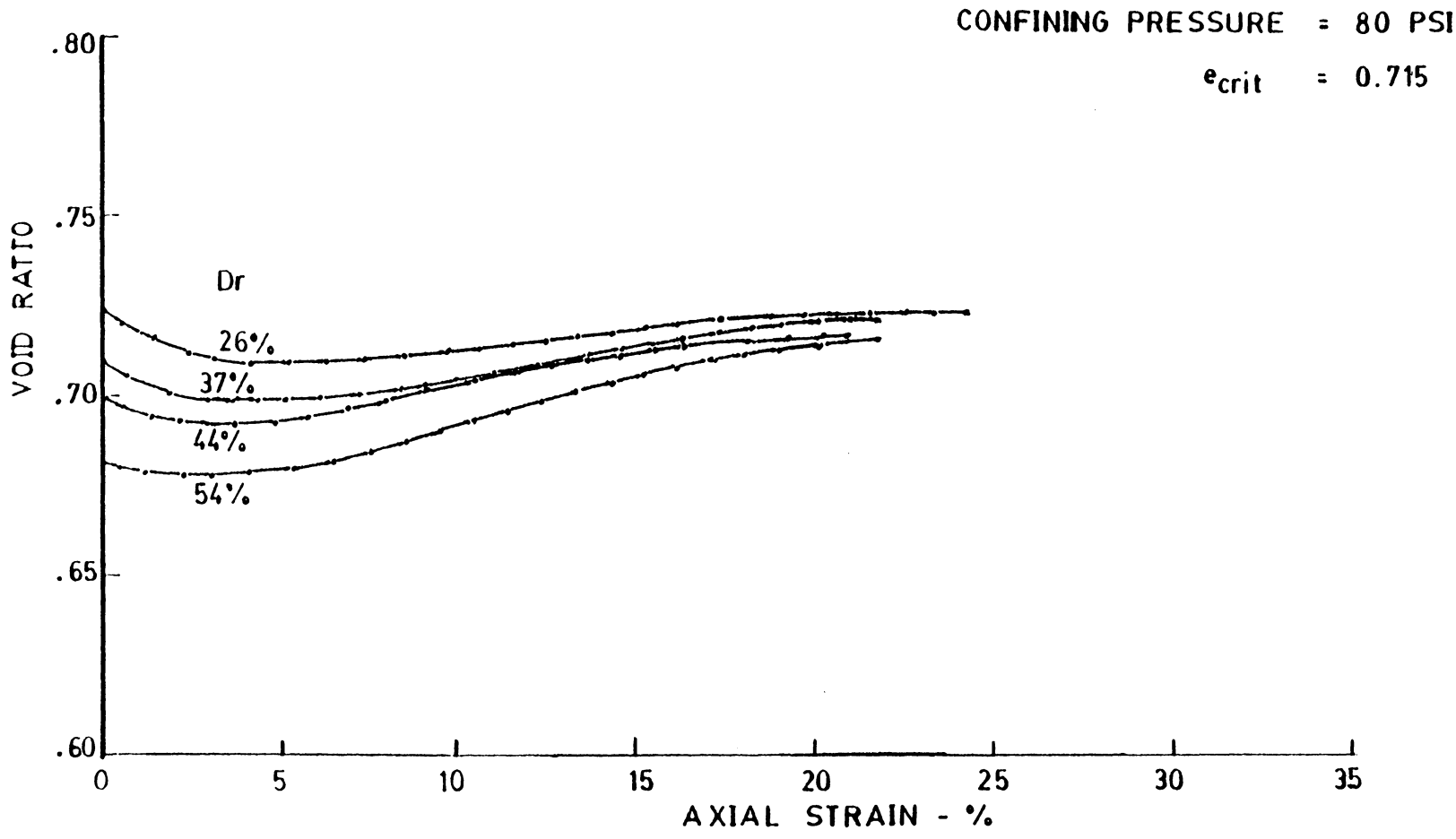

Fig.19 – Void Ratio – Axial Strain Curves for Artificially Cemented Sand with 1 Percent Cement, Confining Pressure = 80 PSI

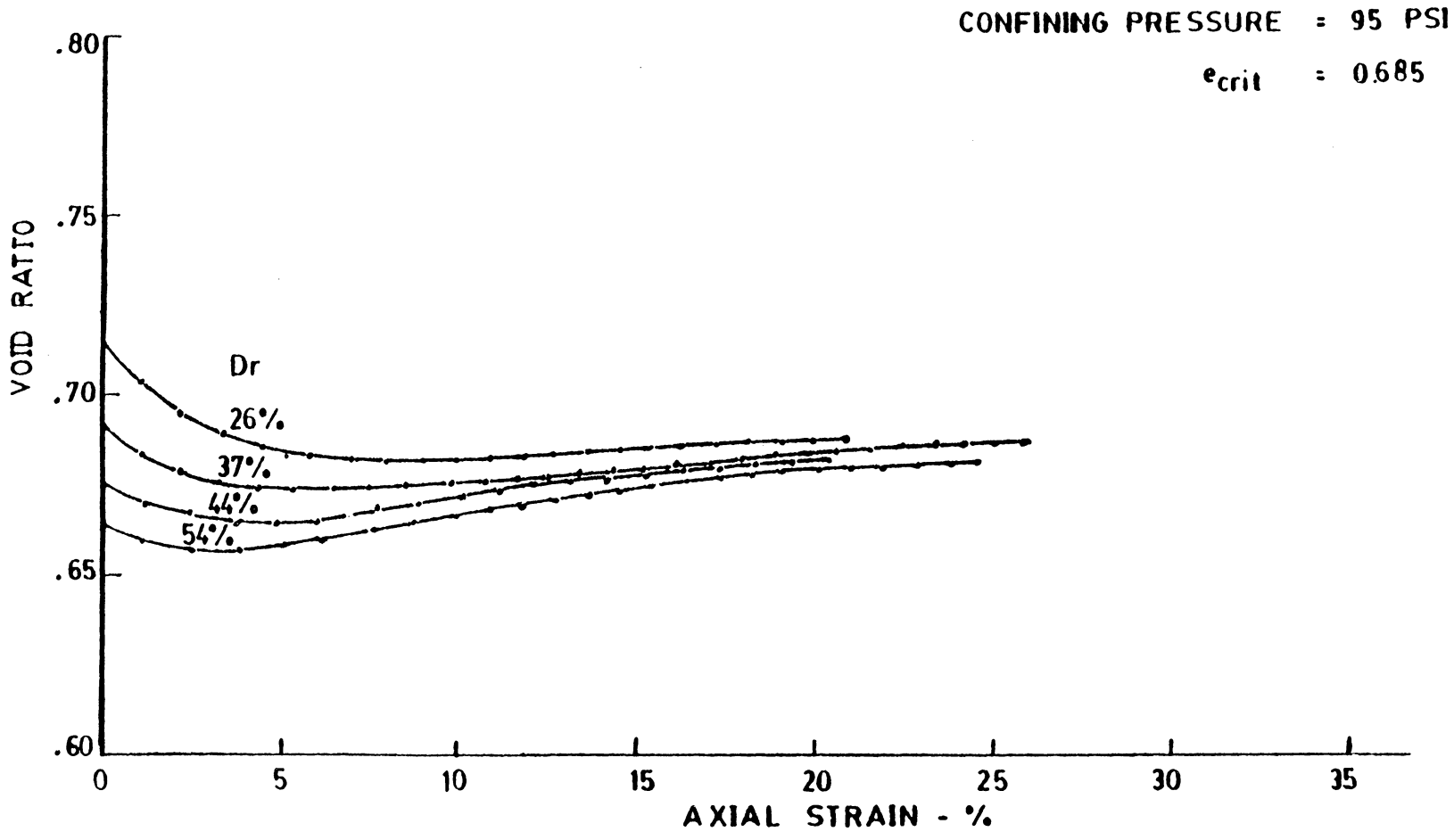

Fig. 20 - Void Ratio - Axial Strain Curves for Artificially Cemented Sand with 1 Percent Cement, Confining Pressure = 95 PSI

7.3 CRITICAL CONFINING PRESSURE

By interpolating data for different constant values of the void ratio at the end of consolidation, e_c, the data in Fig.16(b), which shows the volume change at failure as a function of the confining pressure, for the tests conducted on samples having various densities at the end of consolidation. From this figure, the critical confining pressures corresponding to void ratios of 0.66, 0.68, 0.70, 0.72, and 0.74 are determined, and the results are shown below:

e_c	σ_{3crit} (psi)
0.66	125
0.68	94
0.70	78
0.72	67
0.74	60

7.4 CRITICAL STATE LINE

From the results of the volumetric strain at failure-void ratio curves, a plot was made to show the variation of the critical void ratio, e_{crit}, with the magnitude of the confining pressure, as shown in Fig. 21. Similarly, from the volumetric strain at failure-confining pressure curves, a plot was made to show the relationship between the critical confining pressure, σ_{3crit}, and the void ratio after consolidation, e_c,

as shown in Fig. 22. It will be observed that the relationships shown in Figs. 21 and 22 are identical in form. Since both curves are the same, then these relationships are also the relationship between the critical void ratio, e_{crit}, and the critical confining pressure, σ_{3crit}. This defines the Critical State Line, as shown in Fig. 23, of the artificially prepared samples with one percent cement. From this curve, the values of void ratios and confining pressures at which there would be no volume change at failure could readily be determined. An interesting observation on this curve is that, it indicates that for all practical purposes the critical confining pressure and critical void ratio are uniquely related to each other, and are completely independent of the initial void ratio of the sand. For loose sand, the critical void ratio varies considerably with small changes in confining pressure, while for dense sand, small changes in void ratio cause large changes in the critical confining pressure.

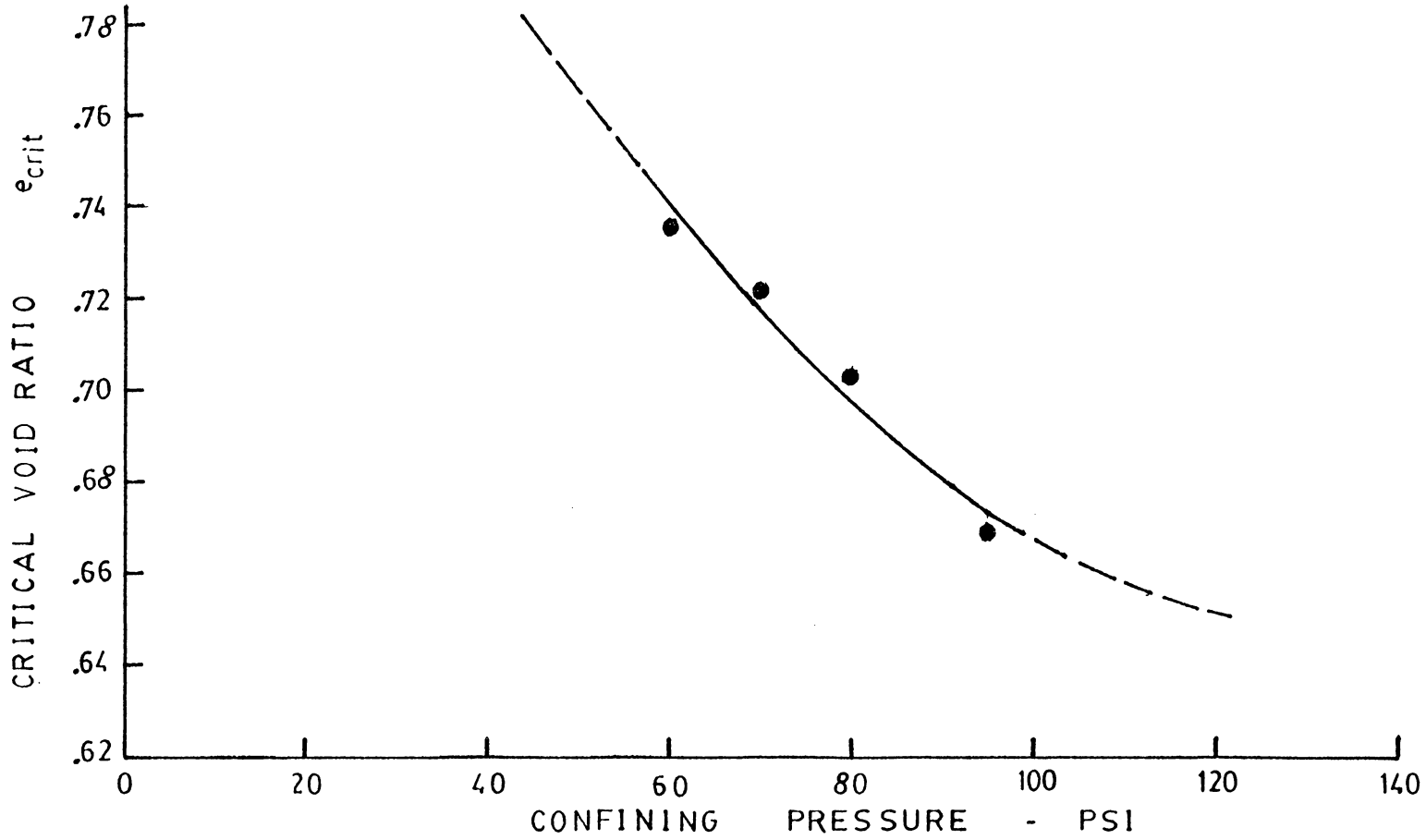

Figure 21: Relationship between Critical Void Ratio and Confining Pressure

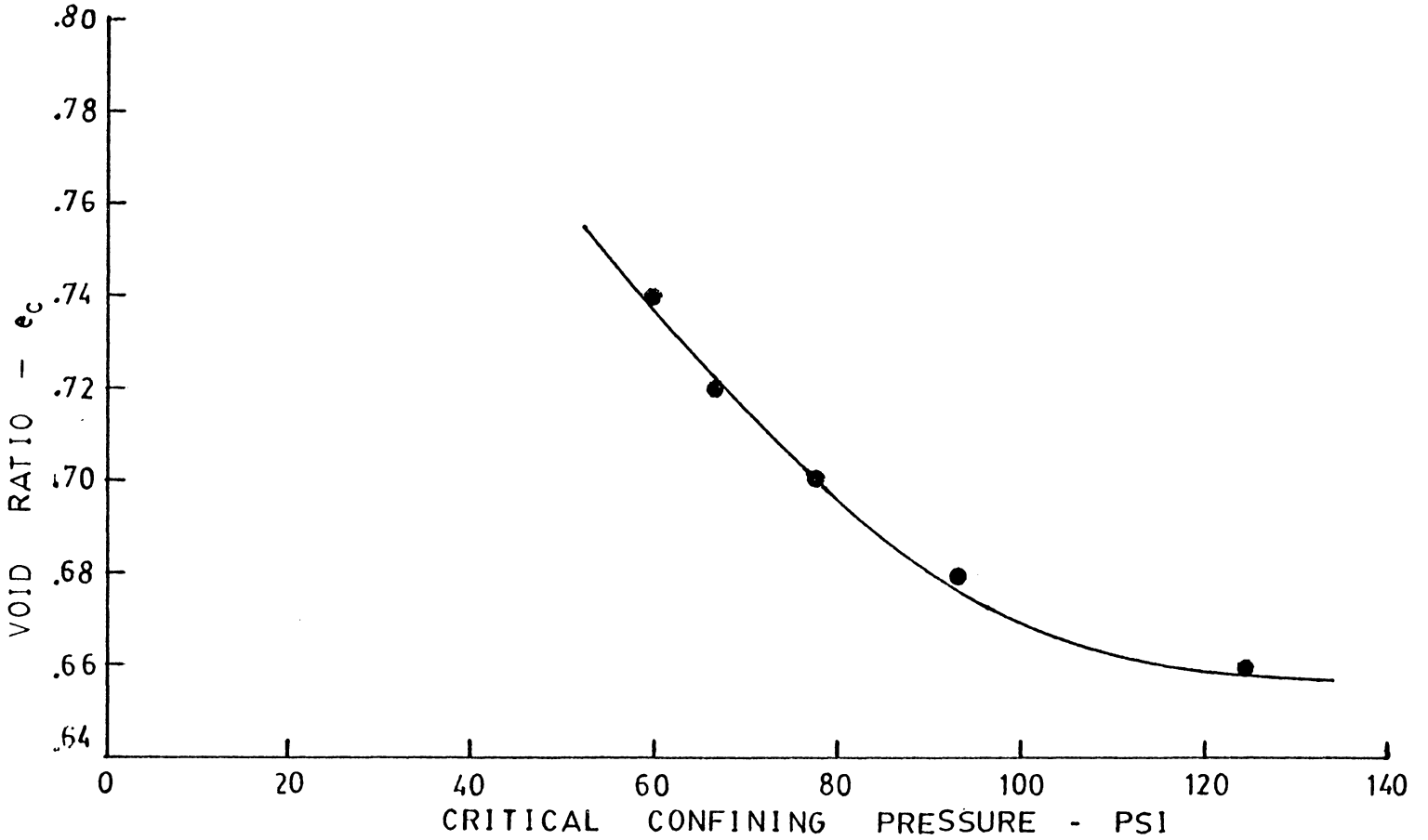

Figure 22: Relationship between Initial Void Ratio and Critical Confining Pressure

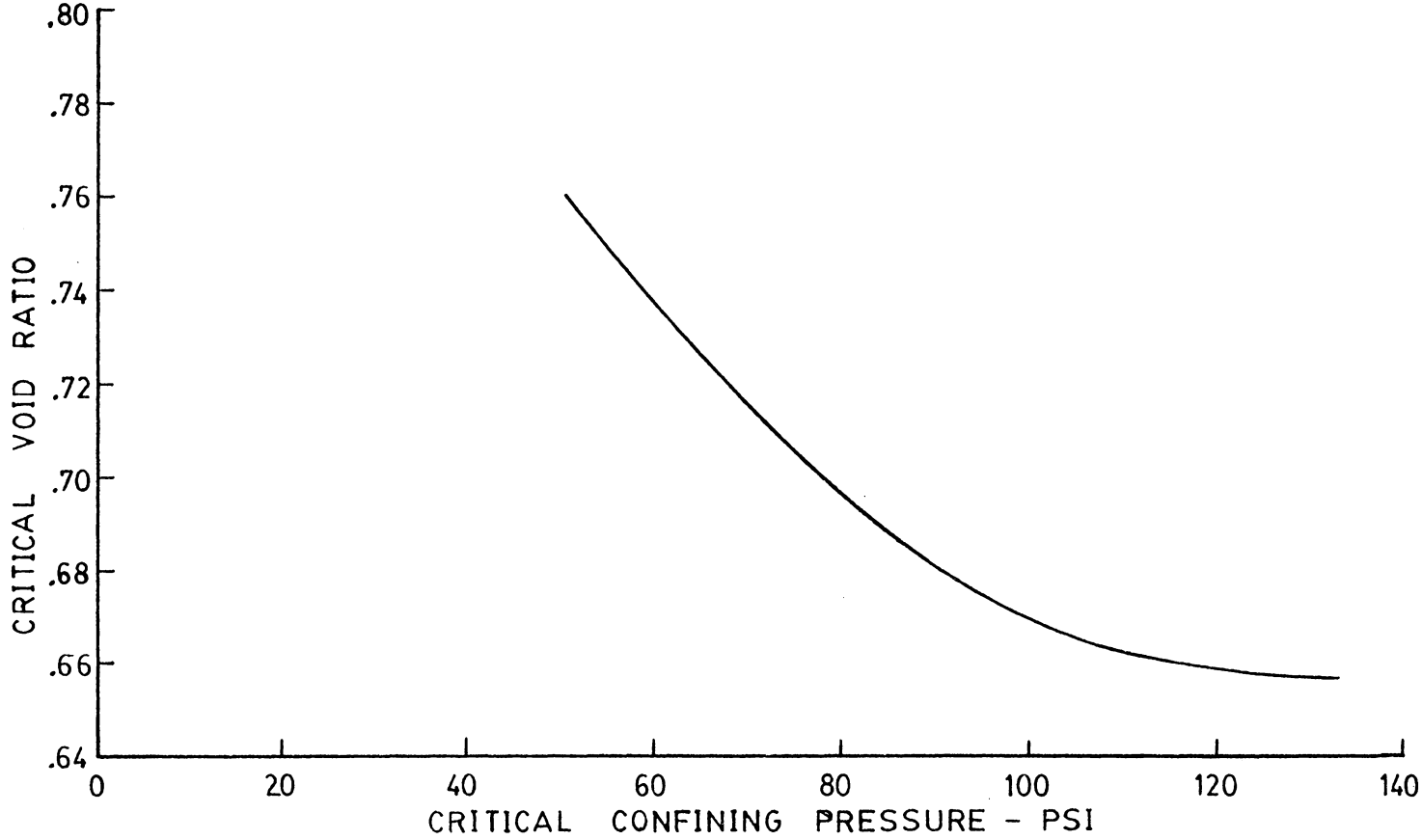

Figure 23: Relationship Between Critical Void Ratio and Critical Confining Pressure

Chapter VIII

SUMMARY AND CONCLUSIONS

This report presents the results of analyzing the critical void ratio concept on weakly cemented sand. The study consists of drained triaxial compression tests performed on artificially cemented sands created to simulate the natural behavior. In order to carry out this study, loose samples were prepared and subjected to different confining pressures such that failure at volumetric contraction could be obtained.

The triaxial test results showed that the samples exhibited similar response to drained loading as compared to previous investigations on the static behavior of naturally and artificially cemented sands.

Following the empirical method of determining the critical void ratio by plotting volumetric strain at failure against void ratio after consolidation, interpolation of the data points yielded critical void ratios of 0.735, 0.722, 0.703 and 0.668 for confining pressures of 60, 70, 80 and 95, respectively. A comparative analysis was made by plotting instantaneous void ratio during the loading against axial strain and this yielded values of 0.745, 0.735, 0.715 and 0.685 for confining pressures of 60, 70, 80 and 95 respectively. However, this method depends on the test accuracies at strain levels beyond 20% where the specimen becomes severely distorted, thus, making this method unreliable to use.

Utilizing the result from volumetric strain-void ratio curves, the relationship between volumetric strain at failure and confining pressure

was plotted and yielded critical confining pressures of 125, 94, 78, 67 and 60 psi for void ratios after consolidation of 0.66, 0.68, 0.70, 0.72 and 0.74, respectively.

From the above results, the critical state line, which shows the variation of the critical void ratio, e_{crit}, with the magnitude of the critical confining pressure, σ_{3crit}, was defined for the artificially prepared samples with one percent cement. It would be interesting to compare this result with the critical state line of uncemented samples and of samples with higher amount of cementation.

The critical state concept is very important in evaluating the undrained strength of sands from drained tests data. The reader is referred to reference 7 since this is beyond the scope of this investigation. This concept is also an important study used in determining the liquefaction potential of sands. A paper by Castro [2] reported that liquefaction can only occur in sands that are looser than the critical state. The results of consolidated-undrained static tests will indicate whether the sand is looser or denser than the critical void ratio for the appropriate confining pressure, and thus whether the sand is susceptible to liquefaction.

The reliability of the parameters obtained depends on a very limited number of data points. The author suggests that more tests on a wider range of relative density and confining pressure should be conducted to obtain more data points where a more accurate interpolation or extrapolation could be done. However, the results presented in this report is

hoped to provide useful informations for further studies to be made on the analysis of critical void ratio concept in cemented sands.

BIBLIOGRAPHY

Bachus, R. C., et al., "Behavior of Weakly Cemented Soil Slopes under Static and Seismic Loading Conditions," Volume II, USGS, Contract No. USGS-14-08-0001-18380, Report No.51, July,1981.

Bishop, A. W., and Henkel, D. J., "Measurement of Soil Properties in the Triaxial Test," 2nd ed., Edward Arnold Publishers, Ltd., 1962.

Black, D. K., and Lee, K., "Saturating Laboratory Samples by Back Pressure," January, 1973, pp. 75-92.

Bowles, J. E., "Engineering Properties of Soils and their Measurement," 2nd ed., MacGraw-Hill Book Co., 1978, pp. 141-174.

Dupas, J. M., and Pecker, A., "Static and Dynamic Properties of SandCement," Journal of Geotechnical Engineering Division , ASCE, Volume 105, No. GT3, March, 1979.

Engineering Manual Laboratory Testing, Headquarters, Department of the Army Office of the Chief of Engineers, November, 1970.

Lambe, W. T., and Whitman, R. V., "Soil Mechanics," John Wiley & Sons, Inc., 1969.

Lee, K. L., and Seed, H. B., "Drained Strength Characteristics of Sand," Journal of the Soil Mechanics and Foundations Division, ASCE, Volume 93, No. SM6, November, 1967, pp. 117-141.

Lowe, J., and Johnson, T. C., "Use of Back Pressure to Increase Degree of Saturation of Triaxial Test Specimens," Presented at the 1960 ASCE Research Conference on Shear Strength of Cohesive Soils, Boulder, Colorado, 1960, pp. 819-836.

Mitchell, J. K., "Fundamentals of Soil Behavior," John Wiley & Sons, Inc., 1976, pp. 316-320.

Saxena, S. K., and Lastrico, R. M., "Static Properties of Lightly Cemented Sands," Journal of Geotechnical Engineering Division, ASCE, Volume 104, No. GT12, Proc. Paper 14259, December, 1978, pp. 1449-1464.

REFERENCES

1. Casagrande, A., "Characteristics of Cohesionless Soils Affecting the Stability of Slopes and Earth Fills," Contributions to Soil Mechanics, 1925-1940, Boston Society of Civil Engineers, 1936.

2. Castro, G., "Liquefaction and Cyclic Mobility of Saturated Sands," Journal of Geotechnical Engineering Division, ASCE, Volume 101, No. GT6, June, 1975, pp. 551-569.

3. Clough, G. W., et al., "Cemented Sands Under Static Loading," Journal of Geotechnical Engineering Division, ASCE, Volume 102, No. GT5, May,1976.

4. Head, K. H., "Manual of Soil Laboratory Testing", Volume 2, John Wiley & Sons, 1982.

5. Mitchell, J. K., "The Properties of Cement-Stabilized Soils," paper prepared for Workshop on Materials and Method for Low Cost Road, Rail, and Reclamation Work, Leuro, Australia, 6-10 September, 1976.

6. Rad, N. S., and Clough , G. W., "The Influence of Cementation on the Static and Dynamic Behavior of Sand," Volume II, USGS, Contract No. USGS-14-08-0001-19763, Report No. 59, December, 1982.

7. Seed, H. B., and Lee, K.L., "Undrained Strength Characteristics of Cohesionless Soils," Journal of the Soil Mechanics and Foundations Division, ASCE, No. SM6, November, 1967, pp. 333-360.

8. Silver, M. L.,et al., "Cyclic Triaxial Strength of Standard Test Sand", Journal of Geotechnical Engineering Division, ASCE, Volume 102, No. GT5, May, 1976.

9. Skempton, A. W., "The Pore Pressure Coefficients A and B," Geotechnique, Volume IV, March, 1954, pp. 143-147.